Wave-Induced Stress and the Drag of Air Flow over Sea Waves

PETER A. E. M. JANSSEN

Department of Oceanography, Royal Netherlands Meteorological Institute (KNMI), De Bilt, The Netherlands

(Manuscript received 20 June 1988, in final form 16 November 1988)

ABSTRACT

In this paper we are concerned with the effect of wind-generated, long gravity waves on the air flow. We study this example of resonant wave–mean flow interaction using the quasilinear theory of wind-wave generation. This theory is an extension of the Miles' shear flow instability in that the effect of the gravity waves on the mean wind profile is taken into account as well. The direct effect of air turbulence on the mean wind profile is modeled by a mixing length model.

We present results of the numerical calculation of the steady state wind profile for given wave spectra. Results are found to be sensitive for the parameterization of the high-frequency tail of the wave spectrum.

Following a proposal by Snyder on the fetch or wave age dependence of the Phillips constant, a strong dependence of the drag of air flow over sea waves on the wave age is found.

For young wind sea (small wave age) a strong coupling between wind and waves is found, whereas there is hardly no coupling for old wind sea. This sensitive dependence of the aerodynamic drag over sea waves on the wave age explains the scatter in plots of the experimental observed drag as a function of the wind speed at 10 meters.

Consequences for the coupling of weather and wave models and for remote sensing (e.g., the scatterometer) are briefly discussed.

1. Introduction

Perhaps one of the most intriguing problems in the theory of surface gravity waves is the generation of sea waves by the wind. A great interest in this problem and a considerable controversy has aroused since the publication of Miles' theory of surface wave generation by shear flow instability three decades ago. One of the main reasons for this controversy was that Miles' theory oversimplifies the physical problem by assuming that the air flow is inviscid and that the turbulence does not play a role except in maintaining the shear flow. Also, early field experiments, in particular by Dobson (1971) gave rates of energy transfer from wind to waves that were an order of magnitude larger than predicted by Miles (1957). The measurement of the energy transfer from wind to waves is, however, a very difficult task as it involves the determination of the phase difference between the wave-induced pressure fluctuation and the surface elevation signal. Later, field experiments (Snyder 1974; Snyder et al. 1981; D. Hasselmann et al. 1986) show order of magnitude agreement with Miles' theory, although theory still predicts energy transfer rates that are smaller than measured values, especially for relatively low frequency waves with a phase speed that is about the same as the wind speed at 10 m.

Corresponding author address: Dr. Peter A. E. M. Janssen, KNMI, P.O. Box 201, 3730 AE De Bilt, The Netherlands.

Recently, there have been several attempts to include the effects of the interaction of waves with air flow turbulence. One approach (e.g., see Riley et al. 1982; Al-Zanaidi and Hui 1984; Jacobs 1987) considers the direct effects of small-scale turbulence on wave growth. Mixing length modeling or second-order closure is then assumed to calculate the turbulent Reynolds stresses, but the direct effect of small-scale eddies on wave growth turns out to be small.

Another approach (Nikolayeva and Tsimring 1986) considered the effect of large-scale turbulence (gustiness) on wave growth. These authors applied a so-called kinetic model for fluid turbulence, proposed by Lundgren (1967), to the problem of wind-generated waves and a substantial enhancement of energy transfer due to gustiness was found, especially for those waves with a phase speed comparable to the wind speed at 10 m.

Thus far, we have discussed the linear theory of wind-wave generation. However, the momentum transfer from wind to sea might be considerable so that the associated wave-induced stress may be a substantial amount of the turbulent stress (Snyder 1974; Snyder et al. 1981). Therefore, the velocity profile over sea waves may deviate from the profile of turbulent air flow over a flat plate.

Consequently, the energy transfer from the air to the sea waves will be affected by sea state so that there is a strong coupling between the turbulent boundary layer and the surface waves generated by it.

The dependence of the air flow on the sea waves is

perhaps best reflected by the dependence of the drag coefficient at 10 m height on the so-called wave age. The wave age parameter (to be defined more precisely later) measures the stage of development of the wind sea. "Young" wind sea, related to a wave spectrum with a relative high peak frequency, refers to a sea state where waves have just been generated by wind, while "old" wind sea refers to a saturated sea state, the energy of which hardly changes in time. There is some experimental evidence on the wave age dependence of the drag coefficient (e.g., Donelan 1982). For a fixed wind speed at 10 m height Donelan found that the drag coefficient of air flow over young wind sea is some 50% larger than the drag coefficient over old wind sea.

This wave age dependence of the drag coefficient of the air flow has important consequences for wave prediction models, storm-surge modeling and modeling of the climate. Also, the consequence might be that one has to couple a global wave prediction model (The WAMDI Group 1988) with a weather forecast model. It is therefore the purpose of this paper to determine the wave age dependence of the drag coefficient by means of a theoretical model of the coupling of the air flow with the sea waves generated by it. In addition, we also determine the wave age dependence of the energy and momentum transfer.

The plan of this paper is as follows: in section 2, we shall introduce the definition of the wave-induced stress. In order to get some idea about the relative importance of the wave stress in the boundary layer, we calculate the wave induced stress, using the bight of Abaco parameterization of the growth of waves by wind (Snyder et al. 1981) and using the Phillips spectrum for the surface waves. It is found that the greater part of the wave-induced stress is carried by the medium to high-frequency waves and that, depending on the wave age, the magnitude of the wave-induced stress varies from 10% (old wind sea) to about 100% of the turbulent stress. It is emphasized, however, that this conclusion depends on how sensitive the Phillips constant depends on wave age. In JONSWAP (1973), where it was attempted to fit both laboratory and field data, a rather weak dependence of the Phillips' constant on wave age was found, with the result that the wave-induced stress is independent on wave age. The JONSWAP relation for the Phillips' constant does not, however, fit the field data particularly well, as was already pointed out by Snyder (1974). The relation proposed by Snyder (1974) gives a stronger wave-age dependence of the Phillips' constant and therefore a stronger wave-age dependence of the wave-induced stress. This is in accord with one's intuition and observations (e.g., see Donelan 1982) that young wind sea is rougher than old wind sea. Nevertheless, a strong impact of growing surface waves on the air flow above it has to be expected. The coupling of wind and waves was considered by Miles (1965), Fabrikant (1976) and Janssen (1982). For one-dimensional propagation it was found that the effect of the waves on the wind profile was similar to the effect of molecular viscosity. For a turbulent wind the evolution of the wind speed U_0 in time t is therefore given by (see section 3)

$$\frac{\partial}{\partial t} U_0 = \nu \frac{\partial^2}{\partial z^2} U_0 + \frac{\partial}{\partial z} \tau_t, \quad \nu = \nu_a + D_w \qquad (1)$$

where ν_a is the viscosity of air, D_w is the wave diffusion coefficient (it therefore depends on the wave spectrum), z is the height above the water surface and τ_t is the turbulent stress.

It should be emphasized, however, that the evolution equation (1) only has a restricted validity as it is based on the Miles' resonance mechanism, thus effects of molecular viscosity and air turbulence on the critical layer have not been taken into account. This means that high-frequency waves (with phase speed c less than $5u_*$, where u_* is the friction velocity), which have their critical layer in the viscous sublayer, are not particularly well modeled by Eq. (1). It was therefore decided to parameterize the effect of these high-frequency waves on the wind profile by means of the introduction of a roughness length; we choose the Charnock relation. Hence, in this paper we shall study the effect of long waves (with phase speed c larger than, say, $5u_*$) on the air flow.

The consequences of this model for the coupling between wind waves and the air flow above it will be discussed in section 4. In particular, we look for steady state solutions of Eq. (1) for given wave spectrum and we determine the wave-age dependence of the drag coefficient and the momentum transfer of air flow to the waves. Section 5 summarizes our conclusions.

2. The wave-induced stress

In generating conditions the air flow over wind waves loses momentum to those waves. Hence, in comparison with air flow over a flat plate, the air flow over surface gravity waves feels an additional stress due to the presence of the waves, the so-called wave-induced stress. This stress is most easily determined from the rate of change of the momentum of the waves.

Here, we are only interested in the order of magnitude of the wave momentum so we shall neglect effects of the water current and capillarity on the dispersion relation of the surface waves. The dispersion relation then reads

$$\omega = \sqrt{gk}, \qquad (2)$$

where ω is the angular frequency and g is the acceleration of gravity. Using Whitham's variational principle in combination with Noether's theorem (Whitham 1974) or by direct calculation of the momentum of a fluid (Phillips 1977), the wave momentum $\vec{P}$ is then given by

$$\vec{P} = \rho_w \omega \phi(k) \vec{l}, \ \vec{l} = \vec{k}/k, \qquad (3)$$

where $\phi(k)$ is the surface elevation spectrum and ρ_w the water density. As the wave-induced stress $\vec{\tau}_w$ is given by the rate of change in time of wave momentum due to wind, we have

$$\vec{\tau}_w = \int d\vec{k} \frac{\partial}{\partial t} \vec{P}\Big|_{\text{wind}} . \tag{4}$$

We are mainly interested in the contribution to the stress of the low-frequency waves, as the effect of the high-frequency waves on the air flow will be modeled by a roughness length. For the rate of change of the surface elevation spectrum due to wind one can therefore use the empirical expression proposed by Snyder et al. (1981) and modified by Komen et al. (1984) to accomodate friction velocity scaling,

$$\frac{\partial}{\partial t} \phi\Big|_{\text{wind}} = \gamma\phi \tag{5}$$

where

$$\gamma = \mu\epsilon\omega \max\left(0, \frac{28u_*}{c}\cos\Theta - 1\right).$$

Here, the wind speed is pointed in the x-direction, Θ is the direction in which the waves propagate, c is the phase speed of the wave, ϵ is the ratio of air to water density, and u_* is the friction velocity. From the bight of Abaco data Snyder et al. (1981) infer a mean value of 0.25 for μ.

Since we are only interested in order of magnitudes at the moment, we shall use a very simple spectral shape,

$$\phi(k, \Theta) = \begin{cases} 0, & k < k_p \\ \frac{1}{2}\alpha_p k^{-4} F(\Theta), & k > k_p \end{cases} \tag{6}$$

where the directional distribution $F(\Theta)$ is given by

$$F(\Theta) = \frac{2}{\pi}\cos^2\Theta,$$

and k_p is the peak wave number corresponding to the peak frequency $\omega_p = \sqrt{gk_p}$. The k^{-4} power law was first proposed by Phillips (1958) and is based on wave breaking being the dominant limiting mechanism for the wave spectrum. The introduction of more complicated looking spectra such as that of JONSWAP (1973) is not essential for the discussion that follows.

Substitution of (5) and (6) into (4) results in the following expression for the ratio of wave-induced stress τ_{wx} to the total stress $\tau = \rho_a u_*^2$

$$\frac{\tau_{wx}}{\tau} = \alpha_p \frac{\mu}{\pi}(28)^2\{f(X_p) + X_p g(X_p) - (X_p)^2 h(X_p)\}, \tag{7}$$

where $X_p = c_p/28u_*$ (here c_p/u_* is the wave age) is a measure for the stage of development of the wind sea, $c_p = \omega_p/k_p$ is the phase speed of the peak of the spectrum, and the functions f, g and k are given (for $X_p \leqslant 1$) by

$$f(X_p) = \frac{16}{15} - (1 - X_p^2)^{1/2}\left(\frac{16}{15} + \frac{8}{15}X_p^2 + \frac{6}{15}X_p^4\right)$$

$$g(X_p) = \frac{3}{2}\arccos(X_p) + 2X_p(1 - X_p^2)^{1/2}\left(\frac{1}{2} + X_p^2\right)$$

$$h(X_p) = \frac{4}{3}\left(1 + \frac{1}{2}X_p^2\right)(1 - X_p^2)^{1/2} \tag{8}$$

and for $X_p \geqslant 1$ these functions take the values $^{16}/_{15}$, 0, 0, respectively. Note that by symmetry the y-component of the wave stress is zero.

The order of magnitude of the ratio of wave-induced stress to turbulent stress is then found to vary between 0.20 and 1 or even larger. However, this estimate of τ_w depends largely on the wave age dependence of the Phillips constant. Following Snyder (1974) one would infer from the standard JONSWAP fetch laws the relation

$$\alpha_p \sim (c_p/u_*)^{-2/3}. \tag{9}$$

It results in a wave-induced stress that is virtually independent of the waves, as shown in Fig. 1. As noted by Snyder (1974) and Hasselmann et al. (1973), the power law (9), which attempts to cover both laboratory and field data, does not fit the field data particularly well. As a matter of fact, there is no reason to assume that both field and laboratory data may be described by a single power law. A power law that fits the JONSWAP data (and also the KNMI data, see Janssen et al. 1984) well shows a much stronger dependence of α_p on wave age. It is given by

$$\alpha_p = 0.57(c_p/u_*)^{-3/2}. \tag{10}$$

The result is a much stronger wave age dependence of the wave-induced stress, see Fig. 1. We favor the power law (10) because, on the one hand, (10) is in better

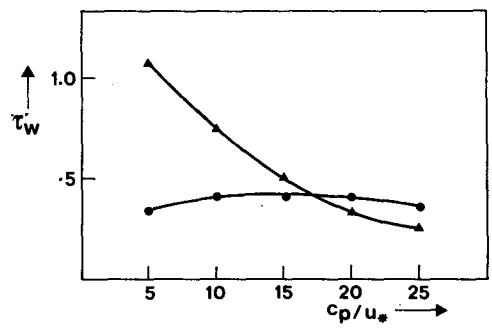

FIG. 1. Wave age dependence of wave-induced stress, normalized with stress $\rho_a u_*^2$, τ'_w, for two different parameterizations of the Phillips' constant: (○) standard JONSWAP law Eq. (9), (△) Snyder's proposal Eq. (10).

agreement with the field data and, on the other hand, the wave-induced stress [based on Eq. (10)] is large for young wind sea ($c_p/u_* = 5$) while small for old wind sea ($c_p/u_* = 30$). The latter is in agreement with one's intuition that air flow over young wind sea is rougher than over old wind sea. Convincing experimental evidence for this is, however, hard to find. Perhaps the results of Donelan (1982) obtained at Lake Ontario under fetch-limited conditions are convincing. Donelan plotted the drag coefficient as a function of wind speed using the wave age as a label. His results are reproduced in Fig. 2, and the plot shows that air flow over old wind sea has a lower drag than over young wind sea. For fixed wind speed, the drag coefficient varies due to the wave-age dependence by a factor of two.

It is conjectured that this variation of the drag coefficient by a factor of two can only be explained if the wave stress has sufficiently sensitive wave age dependence. Returning to Fig. 1 this again supports our choice of the power law (10) for α_p.

From Fig. 1 we infer that, especially for young wind sea, the wave-induced stress is a significant fraction of the total stress. This therefore suggests a strong coupling of the wind and the surface gravity waves. A model for the coupling between wind and waves, based on Miles' shear flow instability mechanism, will be presented in the next section. By means of this model we attempt to study the dependence of the air flow on the presence of the long waves and the impact this might have on the growth rate of the waves by wind. Also, the wave age dependence of the drag coefficient of air flow over growing sea waves is determined.

We finally remark that already Miles (1965) made an attempt to estimate the wave-induced stress, using the Neumann spectrum which has a f^{-6} high-frequency tail. The result was a wave stress of only 20% of the total stress. This led Miles to conclude that the coupling between wind and waves is weak.

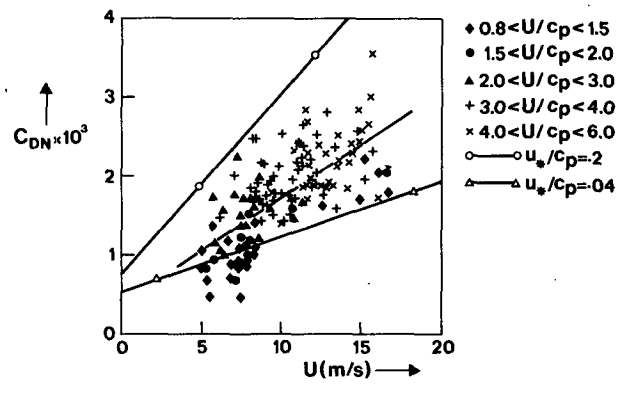

FIG. 2. The observed aerodynamic drag over surface waves as function of the wind speed at 10 meters. The meaning of the symbols, which denote different stages of wave development, is shown in the figure (reproduced with permission of Donelan 1982).

The Neumann spectrum applies, however, to fully developed waves only. Therefore, Miles' estimate should be compared with our estimates for old wind sea (cf. Fig. 1) and a reasonable agreement is then obtained. We again emphasize the importance of the wave age dependence of the high-frequency tail of the spectrum giving rather high energy levels in the high-frequency tail for young wind sea with the result that for underdeveloped wind sea the wave-induced stress is a significant fraction of the total stress.

3. The drag of air flow over sea waves

In this section we study the effect of the waves on the wind profile as we have seen in the previous section that a considerable fraction of the stress τ in the boundary layer over sea is related to the generation of the waves by wind. The coupling of the wind and waves will be investigated by means of the following simple model: The momentum transfer from air flow to the waves is determined by Miles' resonant wave–mean flow interaction so that effects of molecular and turbulent viscosity on the critical layer are disregarded. The neglect of molecular viscosity is justified for the longer waves (with phase speed c larger than $5u_*$, say) which have their critical layer outside the viscous sublayer. The neglect of turbulent viscosity is probably not justified but earlier studies have shown (e.g., see Riley et al. 1982) that the direct effects of small scale turbulence on wave growth are small. Hence, with this model we can only study the effects of the long gravity waves $c > 5u_*$ on the air flow. The effect of the short waves on the wind will be modeled by means of the introduction of a roughness length.

According to Miles' theory of wind-wave generation the rate of change of the surface elevation spectrum $\phi(k)$ due to wind is given by

$$\left.\frac{\partial}{\partial t}\phi\right|_{\text{wind}} = -\pi\epsilon c(k)|\chi_c|^2\frac{W_c''}{|W_c'|}\phi, \qquad (11)$$

where the subscript c refers to evaluation at the critical height z_c defined by $W = U_0 - c = 0$, where $U_0(z)$ is the wind profile, and ϵ is the ratio of air-to-water density. Also, χ is the normalized vertical component of the wave-induced air velocity and it satisfies Rayleigh's equation

$$\left[W\left(\frac{\partial^2}{\partial z^2} - k^2\right) - W''\right]\chi = 0,$$

$$\chi(0) = 1, \quad \chi(\infty) \to 0. \qquad (12)$$

The transfer of momentum from the wind to the waves must be accompanied by a corresponding change of the wind profile. The effect of the waves on the wind profile was determined by Miles (1965), Fabrikant (1976), and Janssen (1982). The wave motion at the surface induces a secondary flow in the air and the vertical and horizontal component of this secondary

flow give rise to a stress that we call the wave-induced stress. As a result the rate of change of the wind velocity due to the presence of the waves is given by

$$\frac{\partial}{\partial t} U_0\Big|_{\text{waves}} = D_w \frac{\partial^2}{\partial z^2} U_0 \tag{13}$$

where the wave diffusion coefficient D_w is proportional to the surface elevation spectrum ϕ,

$$D_w = \frac{\pi c^2 k^2 |\chi|^2}{|c - v_g|} \phi(k), \tag{14}$$

where the wavenumber k has to be expressed as a function of the height through the resonance condition $W = 0$ and v_g is the group velocity $\partial\omega/\partial k$. It is clear that the effect of the waves on the wind profile is analogous to the effect of molecular viscocity. In addition, it should be noted that by use of (11) and (13) the equation for the loss of momentum of the air flow to the waves is found,

$$\frac{\partial}{\partial t}\left(\rho_a \int_0^\infty dz U_0\right)\Big|_{\text{waves}} = -\rho_w \int_0^\infty dk\omega \frac{\partial}{\partial t}\phi\Big|_{\text{wind}} = -\tau_w(z=0) \tag{15}$$

where the right-hand side of Eq. (15) is just the one-dimensional analog of the total wave-induced stress as introduced in Eq. (4). [In passing, it should be noted that we corrected an algebraic error of a factor of 2 in the momentum balance of Janssen (1982).] It is of interest to know what part of the spectrum is affecting the wind profile the most.

This is most easily investigated by introducing a height-dependent wave-induced stress in the following manner

$$\tau_w(z) \equiv -\rho_a \frac{\partial}{\partial t} \int_z^\infty dz U_0(z)\Big|_{\text{waves}} = +\rho_w \int_0^{k(z)} dk\omega \frac{\partial}{\partial t}\phi\Big|_{\text{wind}}, \tag{16}$$

in other words, the rate of change in time of the mean flow momentum in a column starting at z and extending to infinity is given by the rate of change of wave momentum of the low wavenumber part of the spectrum determined by $k < k(z)$. It is emphasized that we have this one-to-one correspondence between z-space and k-space because of the resonant wave–mean flow interaction, hence the wave number $k(z)$ follows from $W = 0$.

The consequences of the effects of the waves on the wind profile have been discussed by Fabrikant (1976) and Janssen (1982). These authors disregarded the effects of molecular viscosity and air turbulence on the wind profile. In this paper we intend, just as Miles (1965) did, to consider these latter effects as well. Therefore, the rate of change of the wind profile in time is governed by the equation

$$\frac{\partial}{\partial t} U_0 = \nu \frac{\partial^2}{\partial z^2} U_0 + \frac{1}{\rho_a}\frac{\partial}{\partial z}\tau_{\text{turb}}, \quad \nu = \nu_a + D_w \tag{17}$$

where we model the turbulent stress by means of a mixing-length model

$$\tau_{\text{turb}} = \rho_a l^2 \left|\frac{\partial}{\partial z} U_0\right| \frac{\partial}{\partial z} U_0 \tag{18}$$

with the mixing length l given by $l = \kappa z$ (κ is the von Kármán constant). The evolution of U_0 is, hence, determined by two competing mechanisms, namely air turbulence that attempts to maintain a logarithmic wind profile, and the combination of diffusion due to viscosity and surface waves, that tries to maintain a linear wind profile.

The effect of the short gravity waves is not well described by the Miles' instability mechanism as the effect of air turbulence and molecular viscosity will give rise to a considerable broadening of the critical layer. Also, capillary waves might give rise to a considerable contribution to the drag of air flow over sea waves. If one were to consider gravity capillary waves with dispersion relation

$$\omega = \{gk + Tk^3\}^{1/2}$$

instead of the dispersion relation (2), then our theoretical model for wave diffusion will certainly fail for those waves in the vicinity of the minimum of the phase speed at $k = \sqrt{g/T}$. This is because at the minimum of the phase speed, where the phase speed c equals the group velocity $\partial\omega/\partial k$, the diffusion coefficient D_w becomes infinite. One would expect that the introduction of, e.g., molecular viscosity will remove this singularity; however, we will not pursue this problem in this paper as we are mainly interested in the effect of the long waves on the drag of air flow over sea.

From observations at sea (e.g., see Donelan 1982) it is known that even for old wind sea the aerodynamic drag is larger than the aerodynamic drag over a flat plate. This increase in drag must be mainly due to the momentum loss to the gravity capillary waves as the longer gravity waves have such a low energy content (because the Phillips constant α_p is small for old wind sea) that their wave stress may be neglected. It is, therefore, important to take into account the momentum loss to the short gravity waves. As, however, no theory on the wave-induced stress of gravity–capillary waves is available we have to rely on a parameterization. Since the phase speed of these short gravity–capillary waves is much smaller than, say, the wind speed at 10-meters height, the air flow experiences a water surface with more or less stationary perturbations, i.e. the air flow experiences a water surface with a certain roughness. Thus, the impact of the short waves is modeled by

means of a roughness length, that is, we impose the boundary condition

$$U_0(z) = 0, \quad z = z_0 \tag{19}$$

where following Charnock (1955), we take as roughness length

$$z_0 = \alpha u_*^2/g, \tag{20}$$

with $\alpha = 0.0144$. A different choice of roughness length (e.g., the relation of Hsu 1974) has hardly no effect on the results regarding the drag coefficient. The steady state solution of Eq. (17) with boundary condition (19) results for old wind sea (e.g., $D_W \approx 0$) in the observed drag law which shows an approximate linear increase with wind speed (Wu 1982).

Finally, for large heights we impose the condition of constant stress and we assume that the waves have no direct impact on the wind profile at those heights, hence

$$\tau_{\text{turb}} = \rho_a l^2 \left|\frac{\partial U_0}{\partial z}\right| \frac{\partial U_0}{\partial z} = \rho_a u_*^2, \quad z \to \infty. \tag{21}$$

The set of equations (12), (14), (17)–(21) describes the effect of the long gravity waves on the air flow. To close this set of equations we need to specify the wave spectrum $\phi(k)$ since the wave diffusion D_w (14) depends on the spectral shape. Clearly, the evolutions of the wave spectrum and the wind speed are coupled, and in principle one should solve the energy balance equation for the waves (see WAMDI Group 1988) in tandem with the momentum equation for the wind. In this study we shall not pursue this approach, but instead we assume that the wave spectrum is given by an empirical relation (the JONSWAP shape) and we shall concentrate on the effect of the waves on the wind. Hence, the spectral shape is given by

$$\phi(k) = \frac{1}{2}\alpha_p k^{-3} \exp\left\{-\frac{5}{4}\left(\frac{k_p}{k}\right)^2\right\}\gamma^r,$$

$$r = \exp\left\{-\frac{1}{2}[(\sqrt{k} - \sqrt{k_p})/\sigma\sqrt{k_p}]^2\right\} \tag{22}$$

where α_p is the Phillips' constant, k_p is the peak wavenumber, γ is the peak enhancement and σ is the width of the spectral peak. Based on the JONSWAP data we obtain parametric relations for the spectral shape parameters α_p, k_p, γ, and σ in terms of the wave age parameter c_p/u_*. For simplicity, we shall give γ and σ the constant value 3.3 and 0.10, respectively, and $k_p = g/c_p^2$ whereas for α_p we either use Eq. (9) or (10) from section 2.

Given the spectral shape (22) we shall in section 4 search for steady-state solutions of the air flow above sea waves. After presenting the numerical method we shall discuss the effect of waves on the drag of the air flow, on the wind profile and on the growth rate of waves by wind.

4. Results

In this section we present the numerical method to search for steady-state solutions of the air flow over sea waves and we compare results for two different parameterizations of the Phillips' constant as a function of wave age.

We found it convenient to introduce dimensionless variables according to

$$t_* = gt/u_*, \quad z_* = gz/u_*^2, \quad k_* = u_*^2 k/g,$$

$$c_* = c/u_*, \quad U_{0_*} = U_0/u_*, \quad D_{w_*} = gD_w/u_*^3,$$

$$\nu_{a_*} = g\nu_a/u_*^3, \quad \phi_* = g^3\phi/u_*^6. \tag{23}$$

Then, dropping the asterisks, the dispersion relation for the gravity waves simply becomes

$$\omega = \sqrt{k}$$

and in the steady state the set of equations governing the behavior of air flow over sea waves may be written as

$$0 = \nu \frac{\partial^2}{\partial z^2} U_0 + \frac{\partial}{\partial z}\left\{l^2\left|\frac{\partial}{\partial z} U_0\right| \frac{\partial}{\partial z} U_0\right\}$$

$$U_0(z = \alpha) = 0; \quad l^2\left|\frac{\partial}{\partial z} U_0\right| \frac{\partial}{\partial z} U_0 = 1, \quad z \to \infty \tag{24}$$

where $l = \kappa z$, $\nu = \nu_a + D_w$. Here, for gravity waves

$$D_w = 2\pi c(k) k^2 |\chi|^2 \phi(k), \tag{25}$$

where we eliminate the wave number k through the resonance condition $W = U_0 - c(k) = 0$, and where χ follows from the solution of Rayleigh's equation plus boundary conditions

$$W\left(\frac{\partial^2}{\partial z^2} - k^2\right)\chi = W''\chi$$

$$\chi(z = \alpha) = 1, \quad \chi(z \to \infty) \to 0 \tag{26}$$

and the wave spectrum is given by Eq. (22). The growth rate $\gamma = \partial \ln\phi/\partial t$ due to wind was then found using Eq. (11).

In order to solve (24)–(36) we used two grids, a coarse- and a fine-mesh grid. On the fine mesh grid

$$z_{\text{fm}}(i) = \alpha(\exp\{\Delta i/\kappa\} - 1), \quad i = 0, 10\,000, \tag{27}$$

(with $\Delta = 0.01$) we solved Eq. (24) by means of a variable step method giving U_0 and $\partial U_0/\partial z$, and intermediate values were obtained by linear interpolation. The curvature in the wind profile $\partial^2 U_0/\partial z^2$ was then found using Eq. (24). The representation of the wind profile on this fine mesh grid was needed in order to obtain a sufficiently accurate solution of the Rayleigh problem (26).

The Rayleigh problem was solved for a relatively small number of waves, because its solution is expensive in terms of cpu units. We generated a set of wavenumbers by specifying the critical height according to

$$z_c(i) = \alpha[\exp(i/\kappa) - 1], \quad i = 1, 25, \quad (28)$$

then the set of wavenumbers followed from the resonance condition $W = U_0 - c(k) = 0$.

It should be realized that we are dealing here with a strongly nonlinear problem as the wave diffusion coefficient D_w depends in a complicated fashion on the wind profile. Therefore, steady-state solutions of (24)–(26) were found by means of an iterative procedure. Denoting the iteration step by a superscript, the starting point for iteration was chosen to be the air flow in absence of gravity waves ($D_w = 0$). This resulted in a first guess for the wind profile $U_0^{(1)}(z)$ which was used in Rayleigh's equation (26) (solved by means of the method of Conte and Miles 1959) to give via Eq. (25) a first guess of the wave-diffusion coefficient $D_w^{(1)}$. To obtain the next guess for the wind profile, we used a mix of the previous wave diffusion coefficient $D_w^{(i-1)}$ and the present value of $D_w^{(i)}$, i.e.

$$\nu^{(i)} = \nu_a + AD_w^{(i-1)} + BD_w^{(i)}, \quad A + B = 1. \quad (29)$$

This was then substituted back into Eq. (24) for the wind profile to give a next guess for $U_0(z)$, and so on.

After some trial and error we found that $A = B = 0.5$ gave a rather rapid convergence to the steady state. The rate of convergence was judged by calculating the total stress

$$\tau_{\text{tot}} = \rho_a\left[\nu_a \frac{\partial}{\partial z} U_0 + l^2\left|\frac{\partial}{\partial z} U_0\right| \frac{\partial}{\partial z} U_0\right] + \tau_w(z) \quad (30)$$

where $\tau_w(z)$ is given by Eq. (16), as in the steady state this is given by its asymptotic value for large z, $\tau_{\text{tot}} = \rho_a$. After 10 iterations we found that this condition was satisfied up to four significant digits.

Steady-state solutions for the wind profile were obtained for two different friction velocities ($u_* = 0.3$ m s^{-1} and $u_* = 0.7$ m s^{-1}) and two different parameterizations of the Phillips' constant α_p [Eq. (9) and Eq. (10)]. We will discuss in detail the case with $u_* = 0.7$ m s^{-1} and a Phillips' constant that depends sensitive on wave age [Eq. (10)].

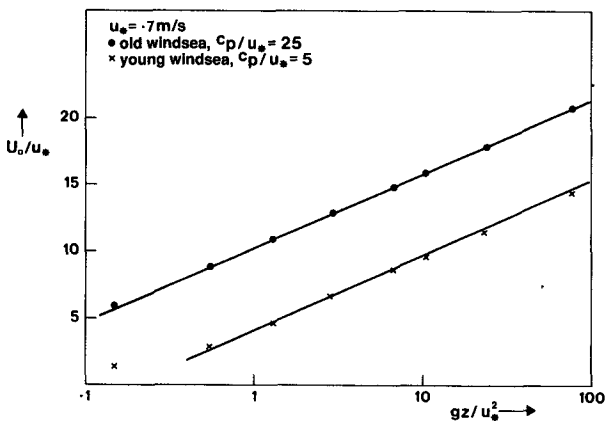

FIG. 3. Dimensionless wind speed as a function of dimensionless height for $u_* = 0.7$ m s^{-1}, showing the effect of long gravity waves on the wind profile for young wind sea ($c_p/u_* = 5$).

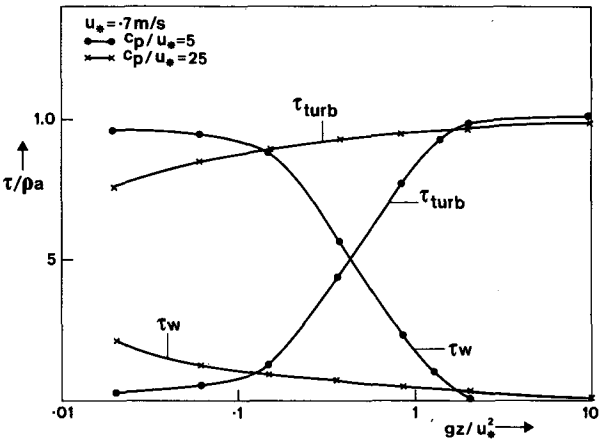

FIG. 4. Distribution of turbulent stress, viscous stress and wave-induced stress as a function of height. The contribution of viscous stress is not shown because it is smaller than 5%.

a. Sensitive dependence of Phillips' constant on wave age (Eq. (10))

The effect of the long gravity waves on the wind profile is illustrated in Fig. 3, where we have plotted the dimensionless wind speed U_0/u_* as a function of dimensionless height gz/u_*^2 for various wave ages. It is clear from this figure that the long waves extract a significant amount of momentum from the air flow, however, young wind sea appears to be rougher than old wind sea. The wind profile is found to be approximately logarithmic except in a region close to the surface ($gz/u_*^2 < 1$), where considerable deviations from the logarithmic profile are found. Even for this large friction velocity this region only corresponds to a few centimeters above the sea surface.

It is of interest to study the distribution of the stress in the boundary layer over turbulence, the wave effect, and viscosity. To this end we have plotted in Fig. 4 the turbulent stress

$$\tau_{\text{turb}} = \rho_a l^2\left|\frac{\partial}{\partial z} U_0\right| \frac{\partial}{\partial z} U_0,$$

the viscous stress

$$\tau_{\text{visc}} = \rho_a \nu_a \frac{\partial}{\partial z} U_0,$$

and the wave-induced stress $\tau_w(z)$ [Eq. (16)] as a function of dimensionless height for young and old wind sea. For young wind sea, we observe that at around $gz/u_*^2 \approx 1$ the wave-induced stress becomes a considerable fraction of the total stress corresponding to the deviations from the logarithmic wind profile in

Fig. 3. At the surface, the stress due to the long waves is then about 95% of the total stress whereas the turbulent stress (which will go into the short waves) is only 5%. In all cases considered, the viscous stress at the surface was quite small; the reason is that by our choice of the Charnock relation as roughness length the water surface is already rough for $\nu_* > 10\alpha$ (or $u_* > 0.1$ m s^{-1}).

On the other hand, for old wind sea the stress going into the long waves is only 35% of the total stress so that most of the stress is supplied to the very short gravity and capillary waves.

Miles (1965) found that the effect of the gravity waves on the curvature of the wind profile was quite small. The reason for this is that he considered old wind sea spectra only. For fully developed waves our results agree with his as the wind profile is then almost identical to the profile in the absence of long waves (cf. Fig. 3 and Fig. 4).

However, also Miles' choice of the high-frequency tail of the spectrum (f^{-6} tail) differs from ours (f^{-5} tail). As a consequence, one should only expect large deviations from the logarithmic profile in a region close to the water surface. This is indeed found in the numerical results, presented in Fig. 3 and Fig. 4.

Referring again to Fig. 1, we have seen that the wave-induced stress obtained from parametrical relations given in section 2 may be a considerable fraction of the total stress or even larger. In Fig. 5 we show what happens according to the quasi-linear theory of wind-wave generation. Here, crosses denote the wave-induced stress calculated from the wind profile in the absence of long waves and diamonds denote the results when there is equilibrium between wind and waves. We infer from the Fig. 5 that for young wind sea the ratio τ_w/τ is reduced considerably, whereas for old wind sea this ratio hardly changes. Apparently, in equilibrium the curvature in the wind profile is for young wind sea reduced in such a way that the ratio τ_w/τ remains less than unity. This must then be accompanied by a considerable reduction of the growth rate of the waves. This is illustrated in Fig. 6 where we plot the normalized growth rate γ/ω of the waves versus the inverse of the dimensionless phase speed c/u_*. Clearly, for fixed phase speed, the growth rate of the waves is larger for old wind sea then for young wind sea. This considerable reduction of the growth rate for young wind sea in the phase speed range $c/u_* > 5$ may be understood by realizing that for rougher air flow (or younger wind sea) and fixed dimensionless phase speed the resonance between wave and air flow occurs at a larger height than for smoother air flow. Consequently, since in this wind speed range the wind profile is logarithmic (see Fig. 3), for fixed phase speed the quantity $W_c''/W_c' \approx 1/z_c$ (where z_c is the critical height) is smaller for young wind sea than for old wind sea. It is emphasized, however, that this is only a partial explanation because a too big reduction of growth rate of the waves for young wind sea would result. To see this, consider again Fig. 3 and compare the critical height for young wind sea with that of the case of no long waves (in practice this is old wind sea). The reduction in growth rate for $c/u_* = 10$ would be about a factor of 6 whereas according to Fig. 6 the growth rate is only reduced by a factor of two. It turns out that the decrease in the curvature of U_0 is accompanied by an increase of the wave-induced velocity in air, χ_c, such that the aforementioned reduction is partly compensated.

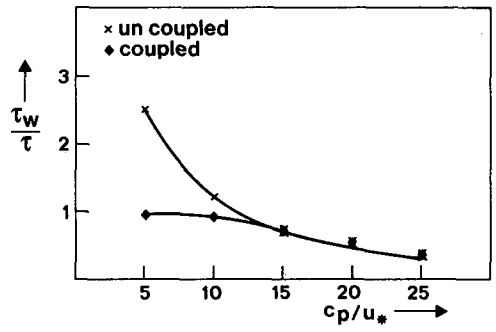

FIG. 5. Reduction of wave-induced stress due to the quasi-linear coupling of wind and waves. Crosses denote the normalized wave stress calculated from the wind profile in the absence of the long waves and diamonds denote results when there is equilibrium between wind and waves.

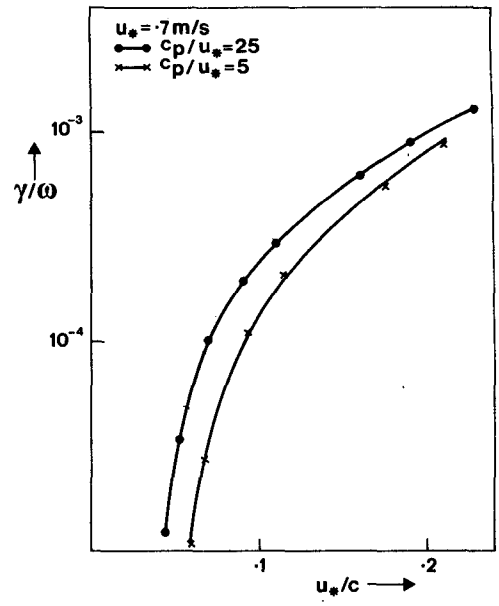

FIG. 6. The normalized growth rate γ/ω of the waves as a function of the inverse of the dimensionless phase speed c/u_* of the waves. The labels refer to different wave age and $u_* = 0.7$ m s^{-1}.

It is concluded that there is a strong coupling between wind and the waves generated by it, especially for young wind sea. This is, on the one hand, reflected by an air flow that is rougher than can be expected from Charnock's relation for the roughness length alone, and, on

the other hand, a strong reduction of growth of the waves by wind for young wind sea. However, it should be remarked that for old wind sea only a very weak coupling between wind and waves is found. There is no need to emphasize that the reason is our choice of dependence of Phillips' constant on wave age. In other words, the high-frequency waves are much steeper for young wind sea than for old wind sea resulting in a larger wave-diffusion coefficient for young wind sea and therefore a rougher air flow for young wind sea than for old wind sea.

We finally remark that a similar conclusion holds for the case $u_* = 0.3$ m s^{-1}. It is no surprise that we find similar results for this case since it was already noted that the consequence of the Charnock relation as roughness length implies a rough water surface already for $u_* \approx 0.1$ m s^{-1}, so that effects of viscosity on the wind profile may be disregarded for larger friction velocities.

b. *Concluding remarks*

We have performed similar calculations for the case that the Phillips' constant only depends weakly on the wave age. It is by now no surprise that both old wind sea and young wind sea give similar effects on the air flow. This is best illustrated by considering the drag coefficient at 10 meters, defined as $c_D(10) = [u_*/U_0(10)]^2$, as a function of wave age c_p/u_*. We have therefore plotted this relation in Fig. 7 for two different friction velocities and the two different parameterizations of Phillips' constant. From this figure the effect of the two different laws for the Phillips' constant is immediate. The standard JONSWAP law for α_p gives hardly no dependence of the drag coefficient on wave age whereas Snyder's proposal results in a sensitive dependence. The implication is that we can now give an explanation of the large scatter found in the field data for the drag coefficient as a function of the wind speed at 10 meters. Returning to Fig. 2 we have shown lines of constant wave age c_p/u_* in the plot of drag coefficient versus wind speed. Using Snyder's proposal for the wave age dependence of the Phillips' constant we find a family of curves that explains the scatter in the field data, whereas the standard JONSWAP relation for α_p would give a single line.

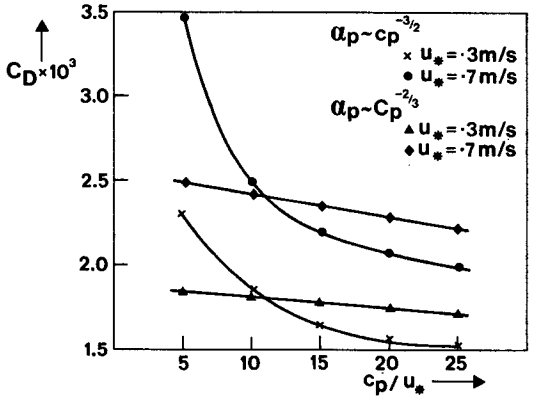

FIG. 7. Aerodynamic drag over sea waves as a function of wave age for two different parameterizations of the Phillips' constant α_p.

We would like to close this section by means of a brief discussion of the impact of the short waves on the air flow, which was modeled by means of a roughness length. It should be remembered that we were forced to introduce this crude parameterization of the effect of the short waves because the Miles' instability mechanism does not take into account, e.g., effects of viscosity. Also, the wave diffusion coefficient D_w becomes infinite at the minimum of the phase speed of the waves. However, a detailed study of the effects of these short waves on the air flow is clearly desirable, if only to understand why Charnock's relation works at all (for an interesting discussion of the topic, see Hasse 1986).

5. Summary of conclusions

In this paper we have studied the effect of wind-generated, long gravity waves on the air flow, where we parameterized the effect of short gravity and capillary waves by means of Charnock's relation. It was found that the coupling between waves and wind was sensitive to how the energy level of the high-frequency waves depends on the wave age. The standard JONSWAP law for the Phillips' constant as function of wave age gave rise to a coupling that is equally strong for both young and old wind sea. On the other hand, Snyder's proposal, which is a better fit to the JONSWAP field data, resulted in a strong coupling for young wind sea and a weak coupling for old wind sea. This is reflected by the strong dependence of the drag coefficient on wave age. Adopting Snyder's proposal for the Phillips' constant as a function of wave age the considerable scatter in the experimental data of drag coefficient as function of wind speed at 10 meters may be attributed to the wave age dependence. For this reason we favor Snyder's proposal.

As a consequence of the coupling between wind and waves we find the growth rate of the waves by wind to be a sensitive function of wave age. This may have important implications for both wave and weather prediction, as the stress in the boundary layer of the atmosphere varies by a factor of two depending on the sea state. Also, the strong coupling between wind and waves may have important consequences for storm-surge modeling as a significant fraction of the momentum and energy of the gravity waves will go to the ocean currents through wave breaking.

Finally, the strong coupling between wind and waves may have significance for the measurement of the windfield over the oceans by means of the so-called scatterometer. Clearly, if one is interested in the wind

speed at 10 meters height and if indeed the energy level of the gravity–capillary waves depends on the friction velocity, the conversion from friction velocity to wind speed has to include the effect of the long waves on the air flow.

Acknowledgments. This work was started at K.N.M.I., continued during a one year stay at ECMWF, Reading, U.K. and finished at K.N.M.I. The author gratefully acknowledges stimulating discussions with Dave Burridge, Anthony Hollingsworth and Liana Zambresky of ECMWF and with Gerbrand Komen of K.N.M.I.

The computations were performed on the Cray XMP-48 of the European Centre of Medium Range Weather Forecasts in Reading.

REFERENCES

Al-Zanaidi, M. A., and W. H. Hui, 1984: Turbulent air flow over water waves. *J. Fluid Mech.*, **148,** 225–246.

Charnock, H., 1955: Wind stress on a water surface. *Quart. J. Roy. Meteor. Soc.*, **81,** 639–640.

Conte, S. D., and J. W. Miles, 1959: On the integration of the Orr–Sommerfeld equation. *J. Soc. Indust. Appl. Math.*, **7,** 361.

Dobson, F. W., 1971: Measurements of atmospheric pressure on wind-generated sea waves. *J. Fluid Mech.*, **48,** 91.

Donelan, M., 1982: The dependence of the aerodynamic drag coefficient on wave parameters. Proc. *First Int. Conf. on Meteorology and Air–Sea Interaction of the Coastal Zone,* The Hague, Amer. Meteor. Soc., 381–387.

Fabrikant, A. L., 1976: Quasilinear theory of wind-wave generation. *Izv. Acad. Sci. USSR, Atmos. Ocean. Phys.*, **12,** 524.

Hasse, L., 1986: On Charnock's relation for the roughness at sea. *Oceanic Whitecaps,* E. C. Monahan and G. MacNiocaill, Eds., 49.

Hasselmann, D., J. Bösenberg, M. Dunckel, K. Richter, M. Grünewald, and H. Carlson, 1986: Measurements of wave-induced pressure over surface gravity waves. *Wave Dynamics and Radio Probing of the Ocean Surface,* O. Phillips and K. Hasselmann, Eds., 353–370.

Hasselmann, K., T. P. Barnett, E. Bouws, H. Carlson, D. E. Cartwright, K. Enke, J. A. Ewing, H. Gienapp, D. E. Hasselmann, A. Meerburg, P. Müller, D. J. Olbers, K. Richter, W. Sell and H. Walden, 1973: Measurements of wind-wave growth and swell decay during the Joint North Sea Wave Project (JONSWAP). *Dtsch. Hydrog. Z.,* **80**(Suppl. A), 12.

Hsu, S. A., 1974: A dynamic roughness equation and its application to wind stress determination at the air-sea interface. *J. Phys. Oceanogr.*, **4,** 116–120.

Jacobs, S. J., 1987: An asymptotic theory for the turbulent flow over a progressive water wave. *J. Fluid Mech.*, **174,** 69–80.

Janssen, P. A. E. M., 1982: Quasilinear approximation for the spectrum of wind-generated water waves. *J. Fluid Mech.*, **117,** 493–506.

——, G. J. Komen and W. J. P. de Voogt, 1984: An operational coupled hybrid wave prediction model. *J. Geophys. Res.*, **89,** 3635–3654.

Komen, G. J., S. Hasselmann and K. Hasselmann, 1984: On the existence of a fully developed wind–sea spectrum. *J. Phys. Oceanogr.*, **14,** 1271–1285.

Lundgren, T. S., 1967: Distribution function in the statistical theory of turbulence. *Phys. Fluids,* **10,** 969–975.

Miles, J. W., 1957: On the generation of surface waves by shear flows. *J. Fluid Mech.*, **3,** 185.

——, 1965: A note on the interaction between surface waves and wind profiles. *J. Fluid Mech.*, **22,** 823–827.

Nikolayeva, Y. I., and L. S. Tsimring, 1986: Kinetic model of the wind generation of waves by a turbulent wind. *Izv. Acad. Sci. USSR, Atmos. Ocean. Phys.*, **22,** 102–107.

Phillips, O. M., 1958: The equilibrium range in the spectrum of wind-generated water waves. *J. Fluid Mech.*, **4,** 426–434.

——, 1977: *Dynamics of the Upper Ocean,* 2nd ed. Cambridge University Press.

Riley, D. S., M. A. Donelan and W. H. Hui, 1982: An extended Miles' theory for wave generation by wind. *Bound.-Layer Meteor.*, **22,** 209–225.

Snyder, R. L., 1974: A field study of wave-induced pressure fluctuation above surface gravity waves. *J. Mar. Res.*, **32,** 497–531.

——, F. W. Dobson, J. A. Elliot and R. B. Long, 1981: Array measurements of atmospheric pressure fluctuations above surface gravity waves. *J. Fluid Mech.*, **102,** 1.

The WAMDI Group, 1988: The WAM Model—a third generation ocean wave prediction model. *J. Phys. Oceanogr.*, **18,** 1775–1810.

Whitham, G. B., 1974: *Linear and Nonlinear Waves,* John Wiley.

Wu, J., 1982: Wind-stress coefficients over sea surface from breeze to hurricane. *J. Geophys. Res.*, **87,** 9704–9706.